# Supplementary Information

# Alkyl chain length influence of the functionalized diethanolamine ligand on the slow relaxation of the magnetization in $\{Co^{III}_3Dy^{III}_3\}$

**Chlöe Bonnenfant[a,b], Nahir Vadra[a], Mathieu Rouzierès[c], Rodolphe Clérac[c], Fabio D. Cukiernik[a]* and Pablo Alborés[a]***

[a] Departamento de Química Inorgánica, Analítica y Química Física/ INQUIMAE (CONICET), Facultad de Ciencias Exactas y Naturales Universidad de Buenos Aires, Pabellón 2, Ciudad Universitaria, C1428EHA Buenos Aires, Argentina
Fax: +5411 / 4576-3341
e-mail: albores@qi.fcen.uba.ar; fabioc@qi.fcen.uba.ar

[b] On leave from Ecole Européene d´Ingénieurs de Chimie, Polymères et Matériaux, Université de Strasbourg, France.

[c] Univ. Bordeaux, CNRS, CRPP, UMR 5031, 33600 Pessac, France.

**Table S1**. Main crystallographic data of the reported complexes.

| | **1-$C_4$** | **2-$C_6$** | **3-$C_8$** | **5-$C_{3r}$** |
|---|---|---|---|---|
| Empirical Formula | $C_{59}\,H_{122}\,Co_3\,Dy_3N_4\,O_{29}$ | $C_{65}\,H_{134}\,Co_3\,Dy_3N_4\,O_{29}$ | $C_{71}\,H_{148}\,Co_3\,Dy_3N_4\,O_{30}$ | $C_{46}\,H_{90}\,Co_2\,Dy_2N_2\,O_{18}$ |
| Formula weight | 2014.88 | 2100.04 | 2202.22 | 1402.05 |
| $T$ (K) | 293 (2) | 293 (2) | 293 (2) | 293 (2) |
| Crystal system | Monoclinic | Monoclinic | Monoclinic | Monoclinic |
| Space Group | *Cc* | $P2_1/c$ | $P2_1/c$ | $P2_1/c$ |
| $a$ (Å) | 16.3759(4) | 25.5185(18) | 28.532(2) | 16.1479(5) |
| $b$ (Å) | 19.4907(5) | 19.1773(11) | 10.5787(10) | 14.3681(6) |
| $c$ (Å) | 27.2707(6) | 18.9054(11) | 33.001(3) | 25.5601(8) |
| $\alpha$ (°) | 90 | 90 | 90 | 90 |
| $\beta$ (°) | 90.159(2) | 93.943(6) | 93.753(7) | 93.754(3) |
| $\gamma$ (°) | 90 | 90 | 90 | 90 |
| $V$ (Å$^3$) | 8704.2(4) | 9229.9(10) | 9939(1) | 5917.6(4) |
| $Z$ | 4 | 4 | 4 | 4 |
| $D_{calc}$ (mg/m$^3$) | 1.538 | 1.511 | 1.472 | 1.574 |
| Absorption coefficient (mm$^{-1}$) | 3.171 | 2.994 | 2.785 | 3.111 |
| $F$(000) | 4056 | 4252 | 4484 | 2840 |
| λ( Å) | 0.71073 | 0.71073 | 0.71073 | 0.71073 |
| $\theta$ Range data collection (°) | 3.3 – 27.0 | 3.7 – 23.0 | 3.6 – 27.0 | 3.7 – 27.0 |
| Index ranges | $-20 \le h \le 17$ | $-32 \le h \le 30$ | $-36 \le h \le 36$ | $-20 \le h \le 20$ |
| | $-24 \le k \le 24$ | $-17 \le k \le 24$ | $-13 \le k \le 13$ | $-18 \le k \le 17$ |
| | $-34 \le l \le 34$ | $-24 \le l \le 23$ | $-27 \le l \le 42$ | $-32 \le l \le 31$ |
| Reflections collected/unique | 25479 / 13127 | 41144 / 19693 | 51992 / 21276 | 28678 / 12689 |
| $R_{int}$ | 0.0429 | 0.1111 | 0.1210 | 0.0484 |
| Observed reflections [$I > 2\sigma(I)$] | 10271 | 9691 | 11740 | 8498 |
| Completeness (%) | 99.7 | 99.6 | 99.4 | 99.7 |
| Maximum / minimum transmission | 0.689 /1.000 | 0.534/1.000 | 0.461/1.000 | 0.630/1.000 |
| Data/restraints/parameters | 13127 /668/928 | 19693 /1834/1037 | 21276/819/1097 | 12689/348/615 |
| Goodness-of-fit (GOF) on $F^2$ | 1.017 | 1.059 | 1.057 | 1.039 |
| Final $R$-index [$I > 2\sigma$(I)]/ all data | 0.069/ 0.098 | 0.1788/ 0.2785 | 0.1157/ 0.1882 | 0.0551/ 0.0926 |
| $wR$ index [$I > 2\sigma(I)$] /all data | 0.194/ 0.242 | 0.3750/ 0.4413 | 0.2672/ 0.3355 | 0.1282/ 0.1559 |
| Largest peak and hole (e A$^{-3}$) | 2.415 and -0.987 | 5.356 and -4.911 | 3.488 and -2.504 | 1.912 and -1.601 |
| Weights, $w$ | $1/[\sigma^2(F_o^2) + (0.1410\,P)^2 + 136.5640\,P]$ where $P=(F_o^2+2F_c^2)/3$ | $1/[\sigma^2(F_o^2) + 1274.4493P]$ where $P=(F_o^2+2F_c^2)/3$ | $1/[\sigma^2(F_o^2) + (0.1109\,P)^2 + 192.2491\,P]$ where $P=(F_o^2+2F_c^2)/3$ | $1/[\sigma^2(F_o^2) + (0.0513\,P)^2 + 43.2064\,P]$ where $P=(F_o^2+2F_c^2)/3$ |

**Table S2.** Dy-O bond distances (Å) of reported complexes.

| **1-$C_4$** | | | | | **2-$C_6$** | | | | **3-$C_8$** | | |
|---|---|---|---|---|---|---|---|---|---|---|---|
| | O22 | Dy1 | 2.31(2) | | O9 | Dy1 | 2.25(2) | | O8 | Dy1 | 2.27(1) |
| | O6 | Dy1 | 2.32(2) | | O10 | Dy1 | 2.28(2) | | O9 | Dy1 | 2.29(1) |
| | O8 | Dy1 | 2.34(2) | | O11A | Dy1 | 2.32(2) | | O15 | Dy1 | 2.32(1) |
| | O3 | Dy1 | 2.36(2) | | O16 | Dy1 | 2.33(3) | | O14 | Dy1 | 2.38(1) |
| | O23 | Dy1 | 2.37(2) | | O17 | Dy1 | 2.33(3) | | O26 | Dy1 | 2.38(1) |
| | O9 | Dy1 | 2.37(2) | | O1 | Dy1 | 2.35(2) | | O4 | Dy1 | 2.385(9) |
| | O1 | Dy1 | 2.39(2) | | O3 | Dy1 | 2.36(2) | | O2 | Dy1 | 2.388(9) |
| | O15 | Dy1 | 2.45(2) | | O2 | Dy1 | 2.39(2) | | O3 | Dy1 | 2.40(1) |
| | | | | | | | | | | | |
| mean | | | 2.36(2) | | | | 2.33(2) | | | | 2.35(1) |
| max-min | | | 0.14(2) | | | | 0.14(2) | | | | 0.13(1) |
| | O20 | Dy2 | 2.29(2) | | O8 | Dy2 | 2.22(2) | | O6 | Dy2 | 2.32(1) |
| | O11 | Dy2 | 2.31(2) | | O4 | Dy2 | 2.26(2) | | O20 | Dy2 | 2.32(1) |
| | O10 | Dy2 | 2.34(2) | | O7 | Dy2 | 2.34(2) | | O21 | Dy2 | 2.34(1) |
| | O25 | Dy2 | 2.36(2) | | O24 | Dy2 | 2.37(3) | | O7 | Dy2 | 2.35(1) |
| | O24 | Dy2 | 2.36(2) | | O1 | Dy2 | 2.37(2) | | O18 | Dy2 | 2.37(1) |
| | O1 | Dy2 | 2.38(2) | | O27 | Dy2 | 2.39(2) | | O4 | Dy2 | 2.372(9) |
| | O5 | Dy2 | 2.38(2) | | O25 | Dy2 | 2.41(3) | | O2 | Dy2 | 2.381(9) |
| | O3 | Dy2 | 2.39(2) | | O2 | Dy2 | 2.44(2) | | O1 | Dy2 | 2.40(1) |
| | | | | | | | | | | | |
| mean | | | 2.35(2) | | | | 2.35(2) | | | | 2.36(1) |
| max-min | | | 0.10(2) | | | | 0.22(2) | | | | 0.08(1) |
| | O13 | Dy3 | 2.29(2) | | O6 | Dy3 | 2.15(3) | | O5 | Dy3 | 2.28(1) |
| | O2 | Dy3 | 2.31(2) | | O5 | Dy3 | 2.28(2) | | O10 | Dy3 | 2.29(1) |
| | O18 | Dy3 | 2.32(2) | | O20 | Dy3 | 2.29(3) | | O2 | Dy3 | 2.35(1) |
| | O12 | Dy3 | 2.35(2) | | O21 | Dy3 | 2.34(2) | | O24 | Dy3 | 2.35(1) |
| | O1 | Dy3 | 2.38(2) | | O1 | Dy3 | 2.38(2) | | O11 | Dy3 | 2.36(1) |
| | O9 | Dy3 | 2.39(1) | | O14 | Dy3 | 2.39(2) | | O1 | Dy3 | 2.36(1) |
| | O5 | Dy3 | 2.40(2) | | O3 | Dy3 | 2.44(2) | | O3 | Dy3 | 2.384(9) |
| | O27 | Dy3 | 2.41(2) | | O4 | Dy3 | 2.44(2) | | O25 | Dy3 | 2.42(1) |
| | | | | | | | | | | | |
| mean | | | 2.36(2) | | | | 2.34(2) | | | | 2.35(1) |
| max-min | | | 0.12(2) | | | | 0.29(2) | | | | 0.14(1) |

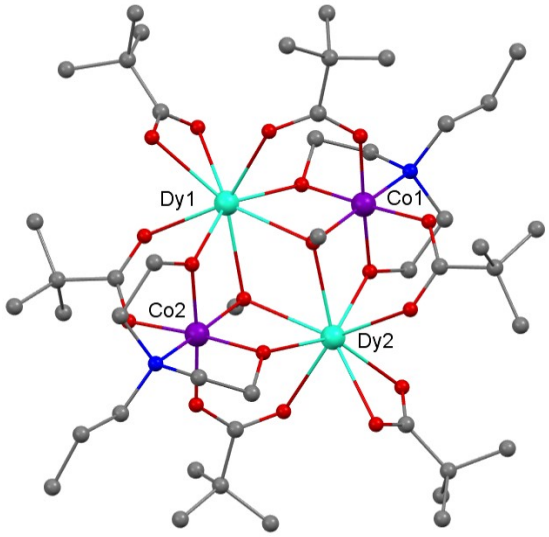


**Figure S1**. Ball and stick molecular representation of complex **5-$C_{3r}$**. Disordered atoms and H atoms were omitted for sake of clarity.

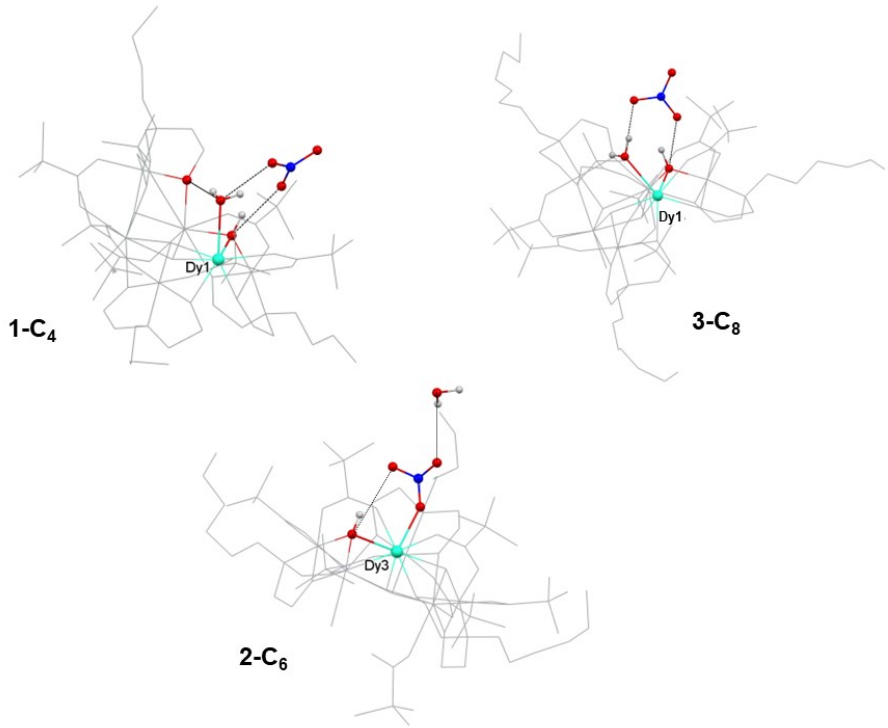


**Figure S2**. Intra-molecular H-bond interaction involving the nitrate ion as ligand and counterion in the reported complexes. Red: O; Blue: N; White: H. Molecule backbone in gray wireframes.

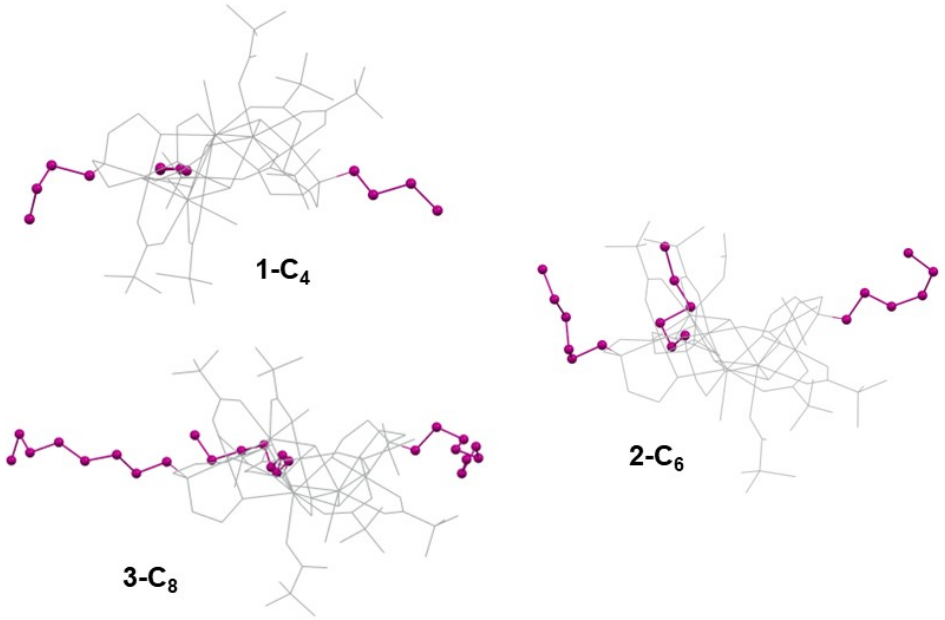


**Figure S3**. Alkyl chains orientation with respect to molecular plane in the reported complexes.

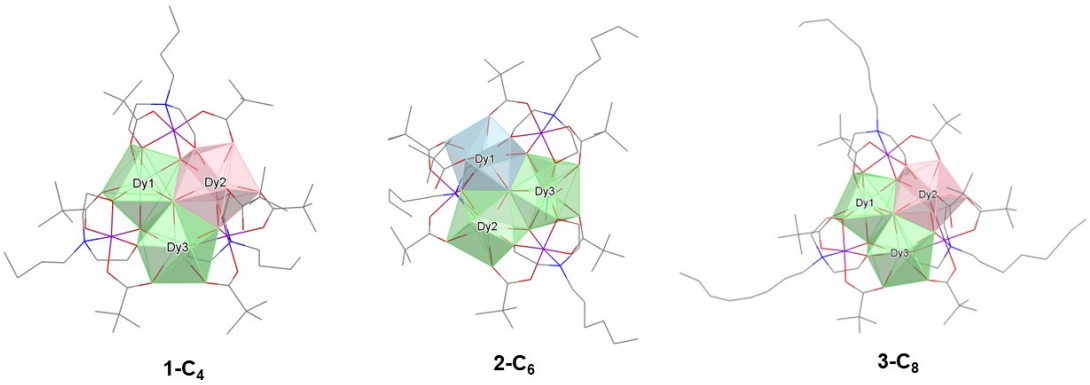


**Figure S4.** Polyhedral representation of Dy(III) sites in the reported complexes. Colours reflect closest geometrical symmetry according to CShM values (see text). Light green: BTP; pink: TDD and light blue: SAP.

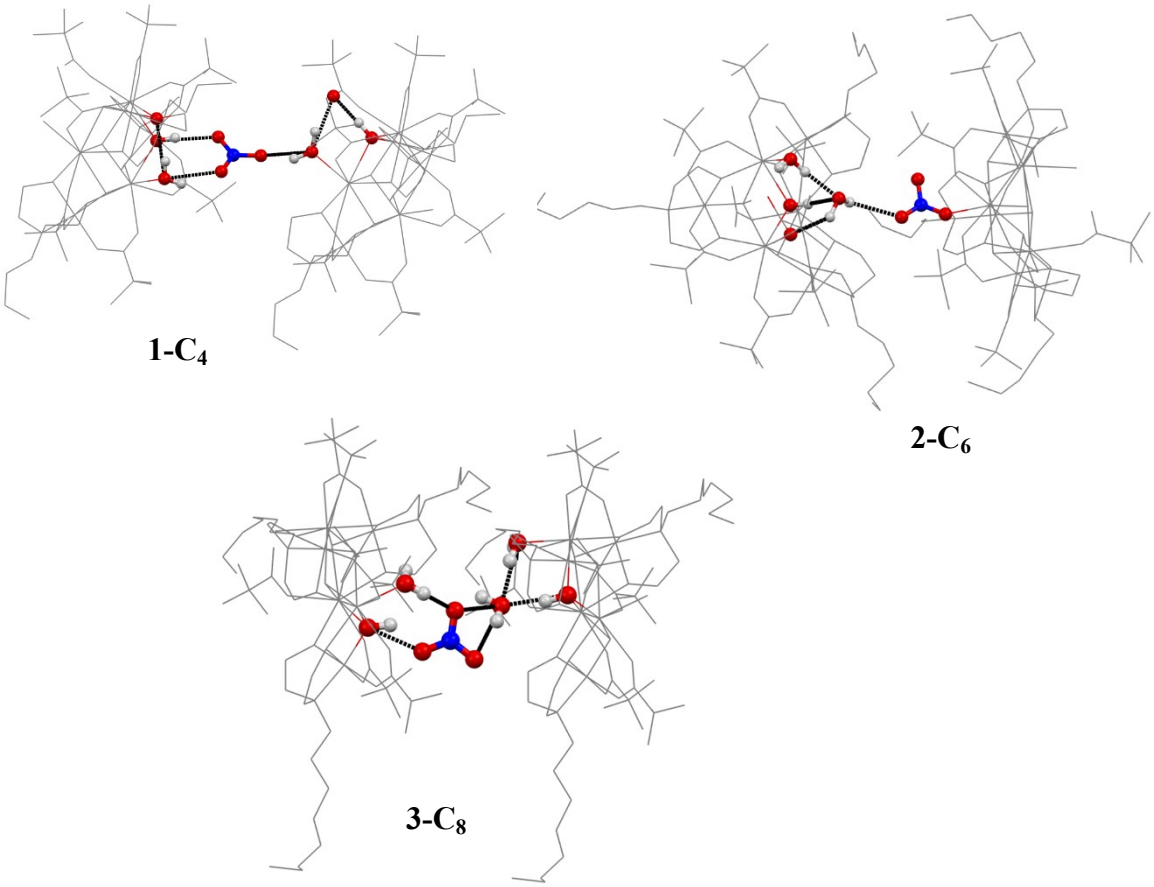


**Figure S5.** Inter-molecular H-interaction mediated by the nitrate counterion (ligand in **2-$C_6$**). H atoms omitted for sake of clarity except for the ones involved in the H-bonding. Red: oxygen; Blue: nitrogen; White: hydrogen.

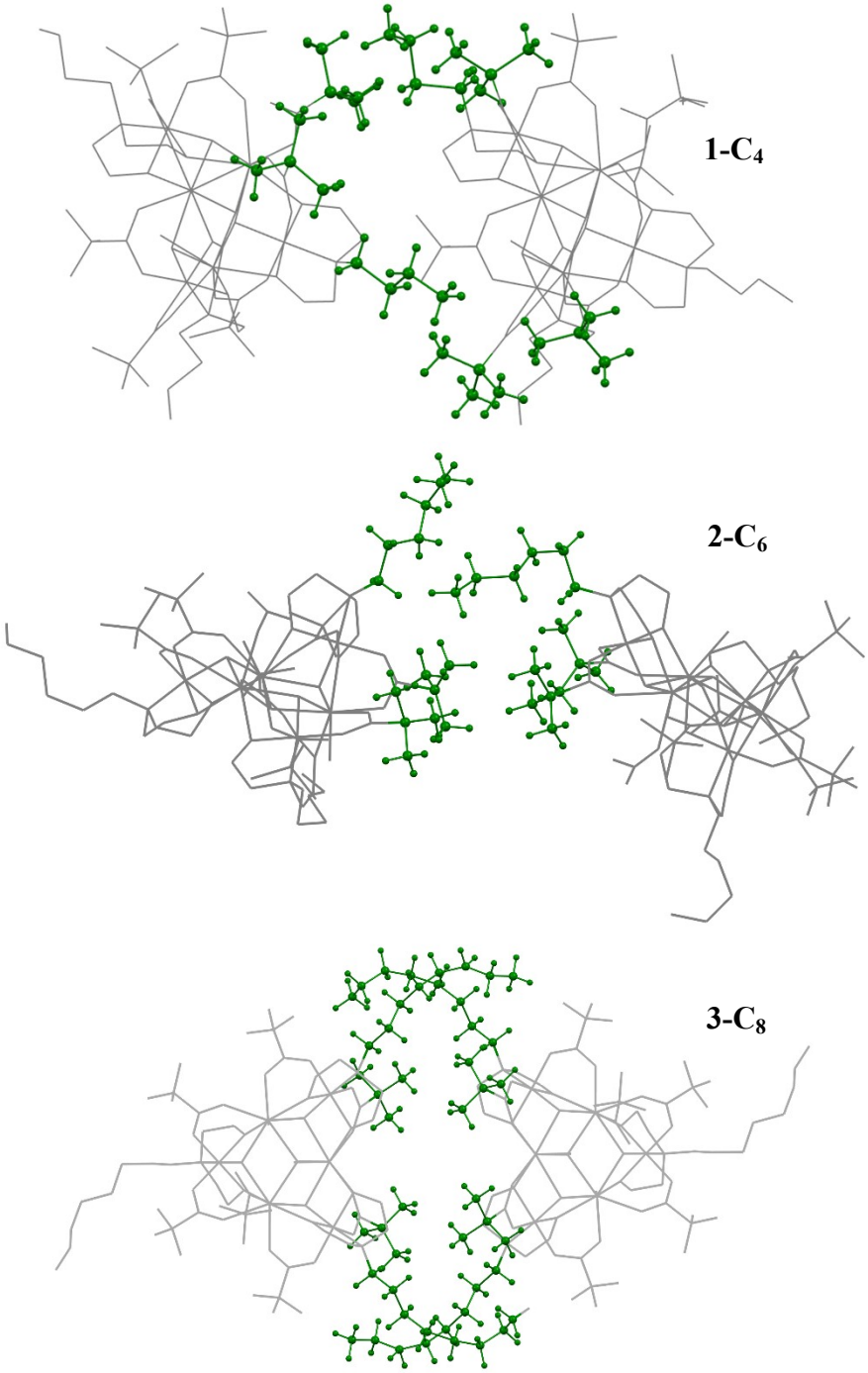


**Figure S6.** Inter-molecular C-H···C-H interactions mediated by the alkyl chains and pivalate *tert*-butyl groups (green). H atoms omitted for sake of clarity except for the ones involved in the inter-molecular interaction.

**1-$C_4$**

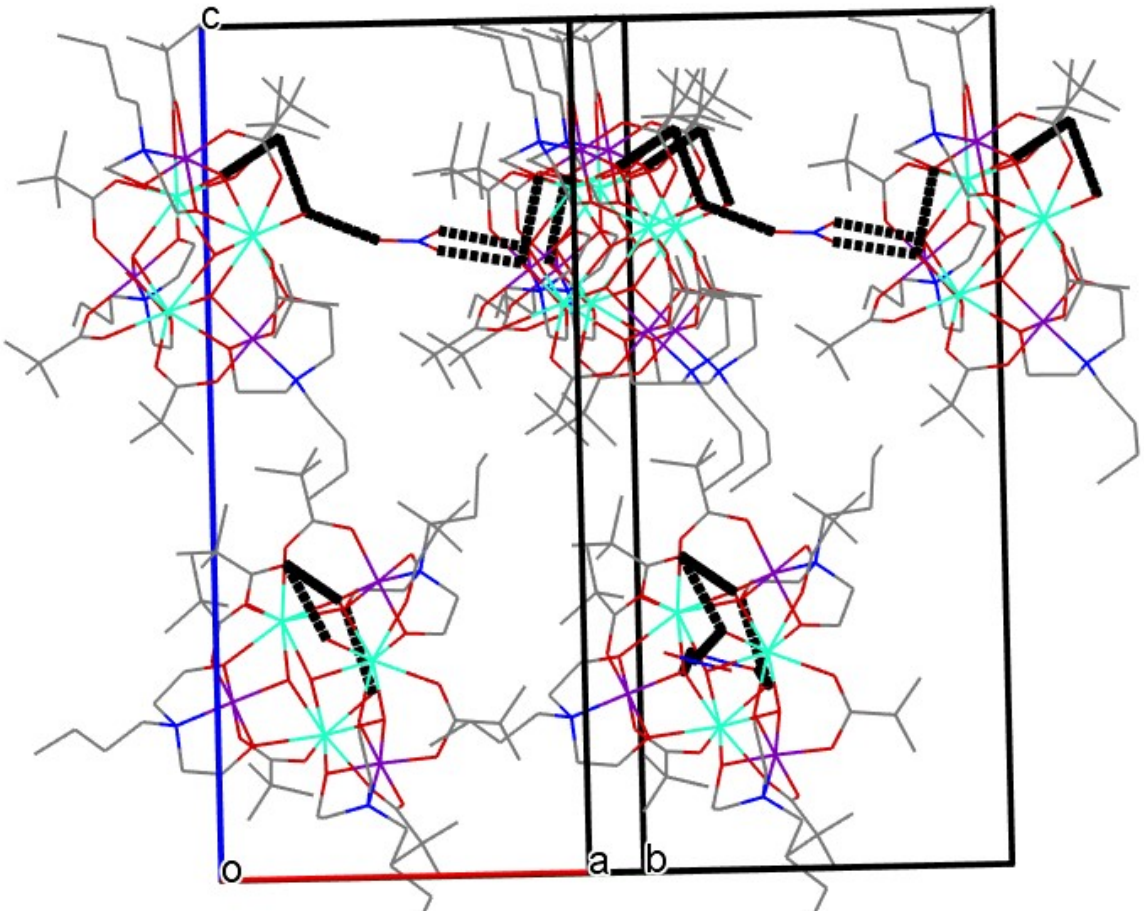


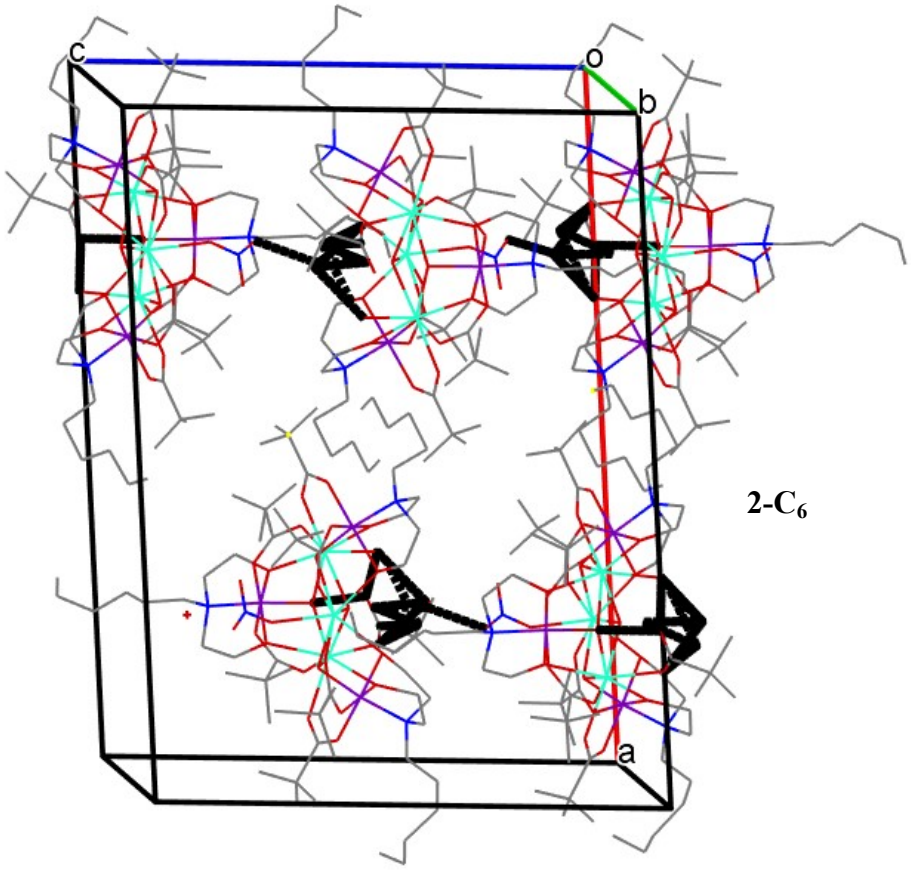


**2-$C_6$**

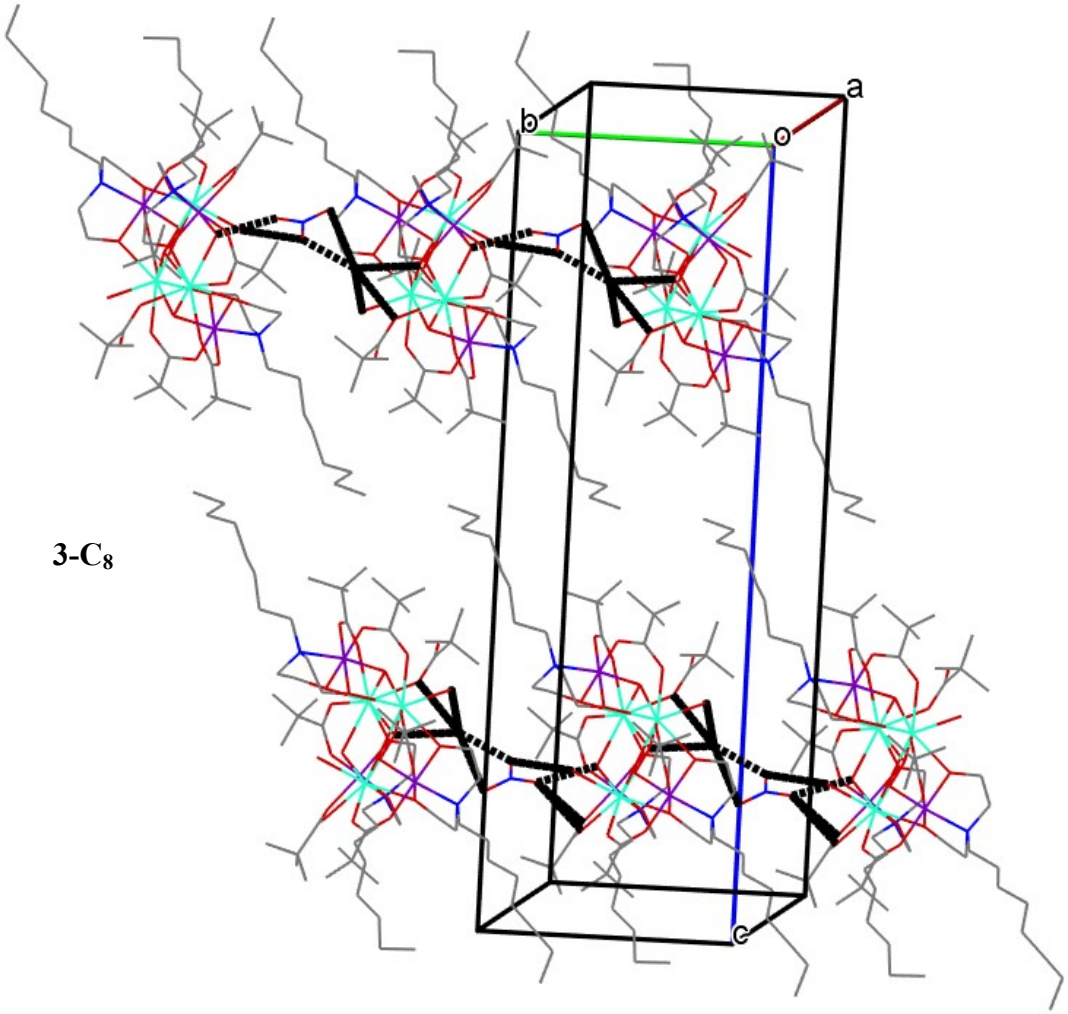


**Figure S7**. Molecular crystal packing showing the H-bond interaction (black dotted lines) and the C-H···C-H ones (black lines). H atoms omitted for sake of clarity.

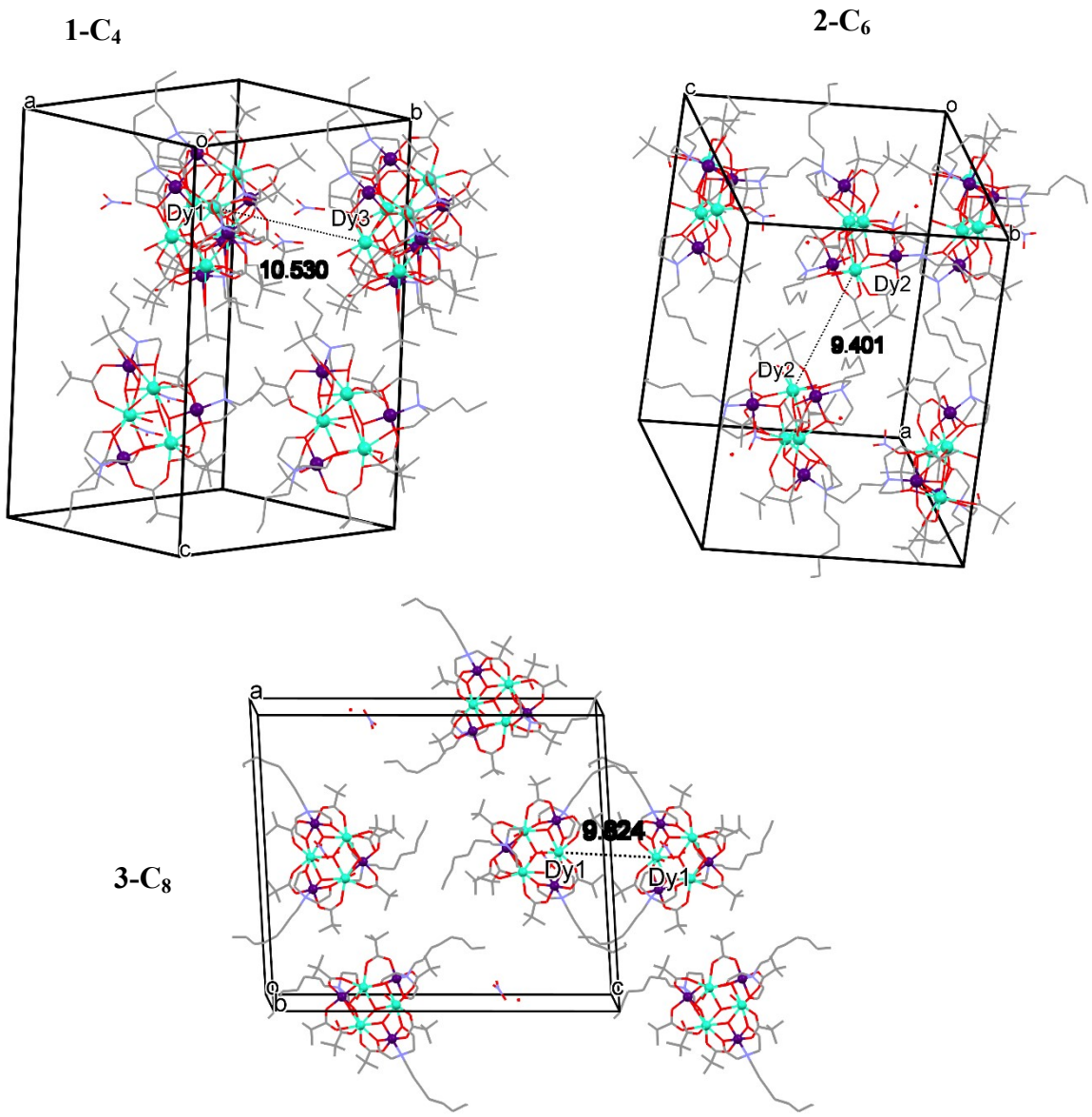


**Figure S8**. Shortest Dy···Dy inter-molecular distances (Å) shown in the crystal packing. H atoms omitted for sake of clarity. Green: Dy; Violet: Co.

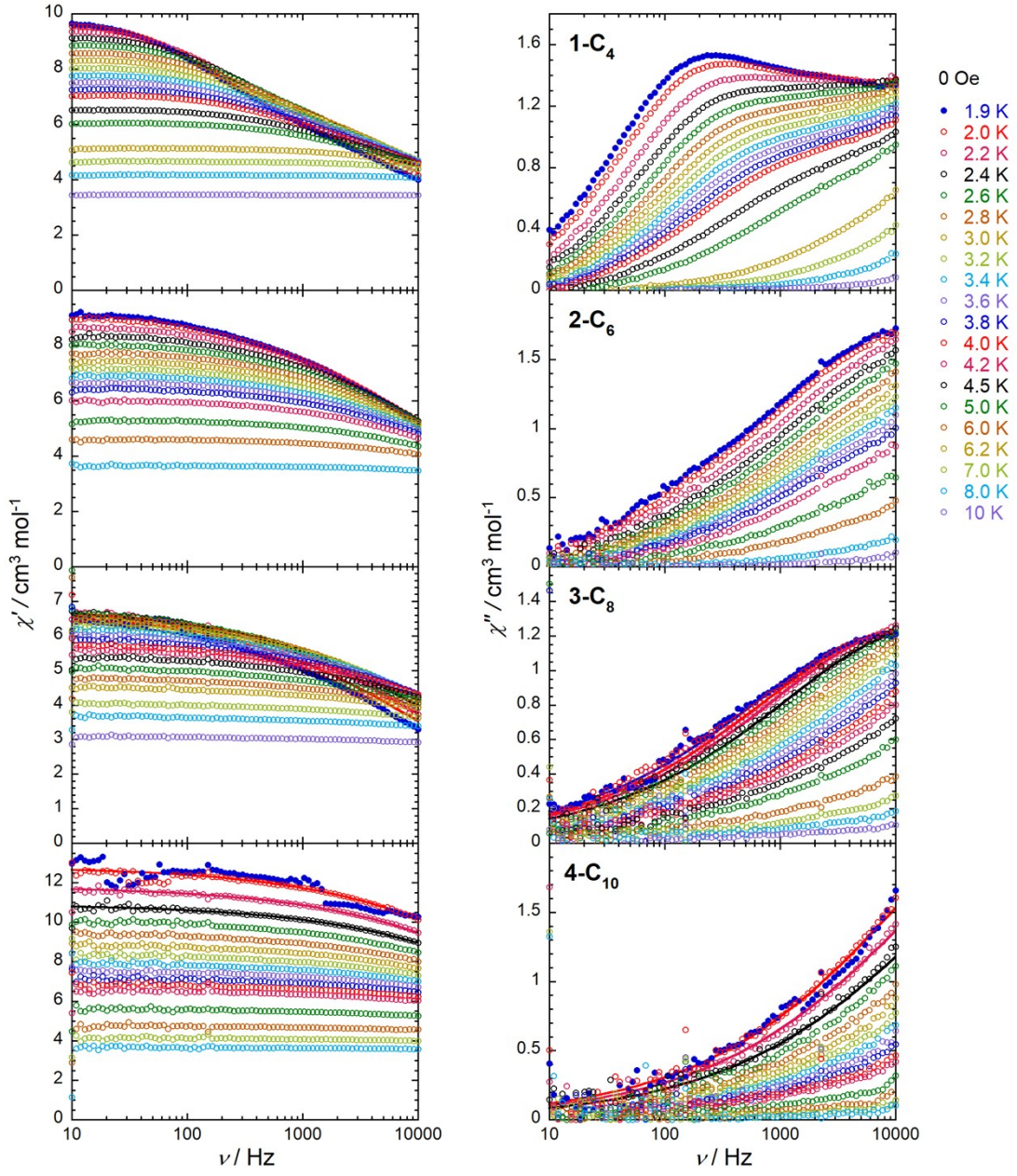


**Figure S9**: Frequency dependence of the in phase (left; $\chi'$) and out of phase (right; $\chi''$) components of the ac susceptibility in zero dc field at indicated temperatures for **1-C$_4$**, **2-C$_6$**, **3-C$_8$** and **4-C$_{10}$**. Solid lines are the best fits to a generalized Debye model.

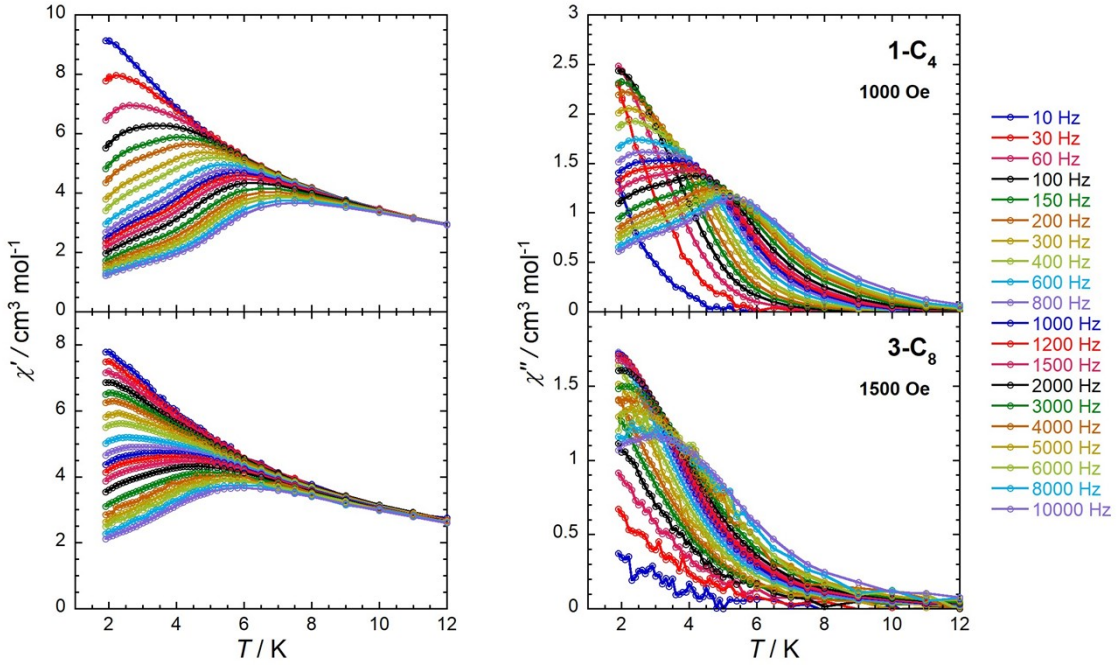


**Figure S10**: Temperature dependence of the in phase (left; $\chi'$) and out of phase (right; $\chi''$) components of the ac susceptibility at optimized dc field and at indicated ac frequencies for **1-C$_4$** and **3-C$_8$**. Solid lines are guide for the eyes.

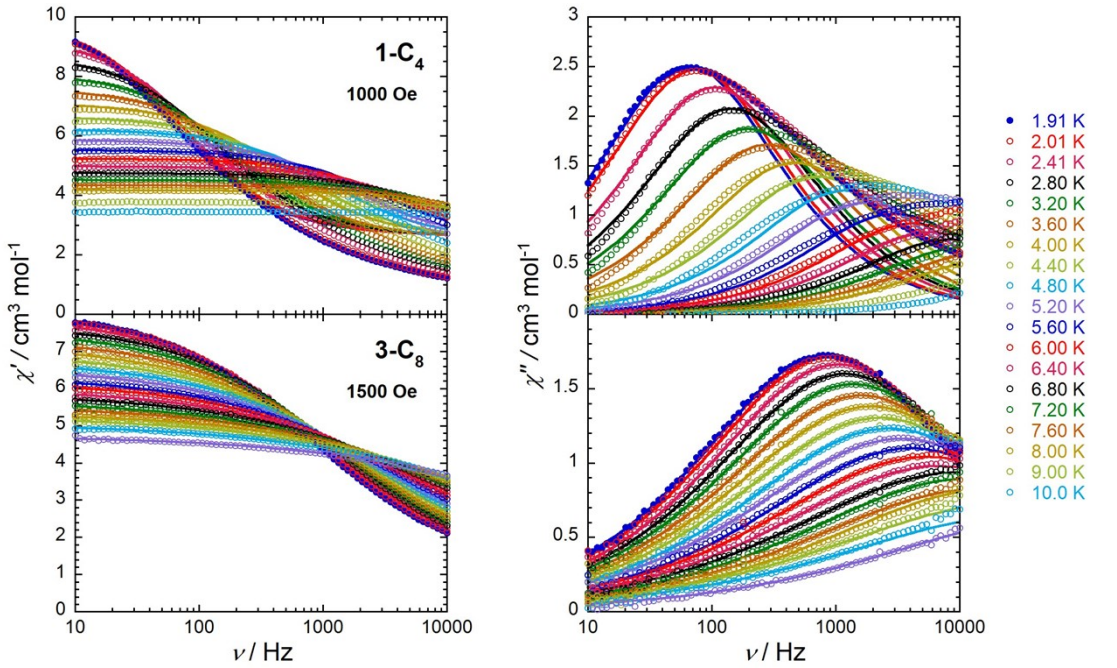


**Figure S11**: Frequency dependence of the in phase (left; $\chi'$) and out of phase (right; $\chi''$) components of the ac susceptibility at optimized dc field and at indicated temperatures for **1-C$_4$** and **3-C$_8$**. Solid lines are the best fits to a generalized Debye model.

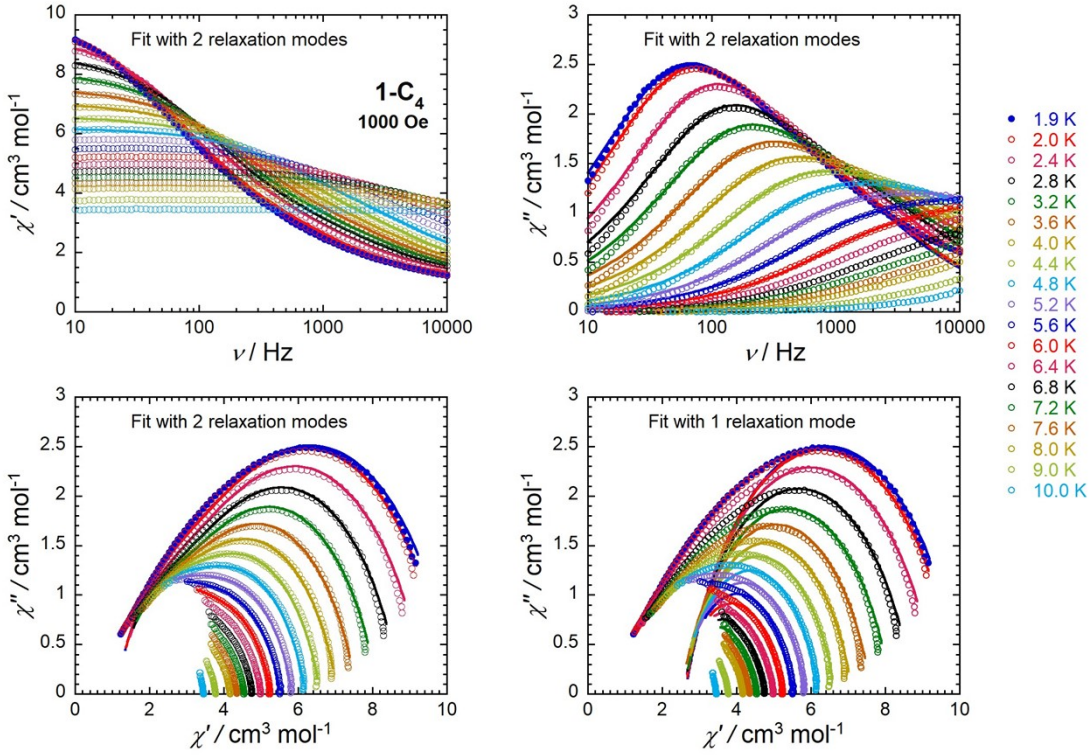


**Figure S12**: Frequency dependence of the in phase (top left; $\chi'$) and out of phase (top right; $\chi''$) components of the ac susceptibility, and the corresponding Cole-Cole plot (bottom left; $\chi''$ vs $\chi'$) where solid lines are the best fits to a generalized Debye model considering two relaxation modes. For comparison, corresponding Cole-Cole plot (bottom right; $\chi''$ vs $\chi'$) where solid lines are the best fits to a generalized Debye model considering a single relaxation mode. All the data are shown at 1000 Oe and at indicated temperatures for **1-C$_4$**.

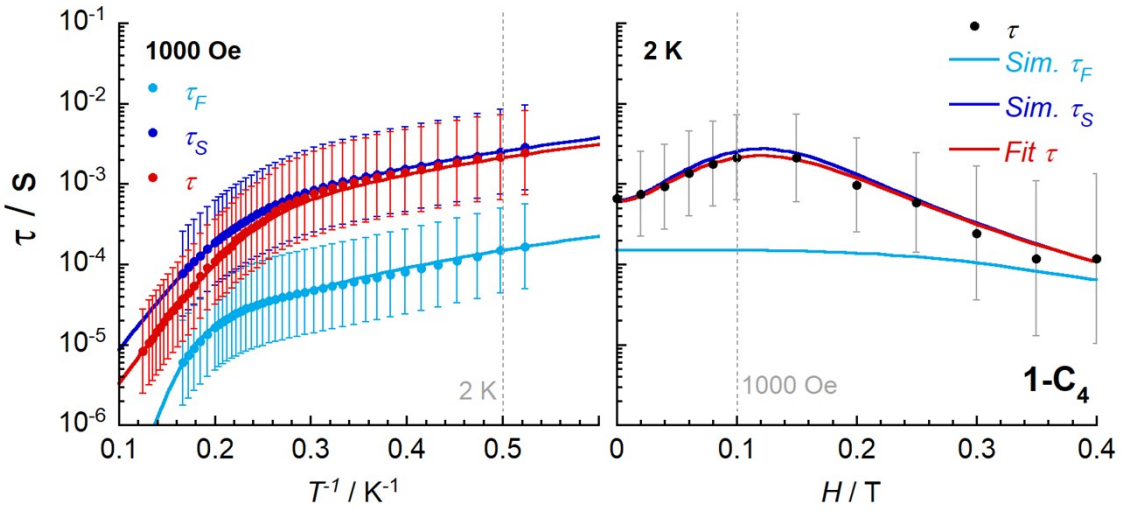

**Figure S13**: Left: Temperature dependence of the relaxation time (plotted as $\tau$ vs $T^{-1}$ in semi-logarith scale) at 1000 Oe for **1-C$_4$**, considering a unique (red dots; $\tau$) and two relaxation modes (blue and light blue dots; $\tau_S$, $\tau_F$). Solid lines are the best fits to these models as discussed in the main text. Right: Field dependence of the relaxation time (plotted as $\tau$ vs $H$ in semi-logarith scale) at 2 K for **1-C$_4$**, considering a unique relaxation mode (black dots; $\tau$). Solid lines are the best fits to the model considering a unique relaxation mode (red line), and simulations with the model considering two relaxation modes (blue and light blue lines; $\tau_S$, $\tau_F$), as discussed in the main text.